

Fig. 2 — Thermo-osmotic permeability of solutions of sodium chloride in water [(○) water, (●) 0.025M, (◐) 0.050M, (×) 0.075M and (◑) 0.100M sodium chloride

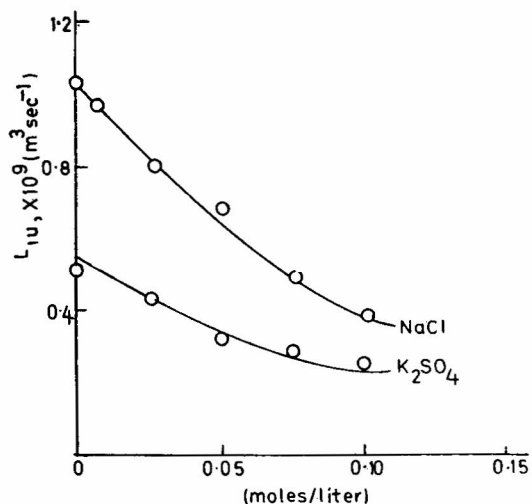


Fig. 3 — Plots of thermo-osmotic coefficient against concentration of the electrolytes

permeability measurement, density of the liquid on the two sides of the membrane was measured after steady state was reached. It was found that density remained practically constant, within experimental error. Density determinations were also made when the flow was allowed to take place under pressure gradient. Again the difference in density on the two sides of the membrane were found to be negligible. Hence it may be concluded that ΔC is negligible.

From these experiments it may be concluded that membrane does not possess semipermeability. This is due to the fact that membrane is not of copper ferrocyanide but of pyrex sinter impregnated with copper ferrocyanide.

It is apparent from Fig. 3 that thermo-osmotic permeability coefficient decreases continuously with increase in concentration of the electrolytes. Thermo-osmosis occurs when the mean free path is comparable to pore diameter, i.e. the thermo-osmotic flow

would be more if the molecules move without undergoing any collision. In the case of electrolytes, water ions are also carried away and they must be hydrated. When the concentration of the ions is increased, the chances of molecular collision during transport would increase and hence thermo-osmotic velocity would diminish with increase in concentration of the electrolytes. The hydrodynamic permeability on the other hand would not depend significantly on concentration of the electrolytes since the viscosity of the aqueous solutions of the electrolytes are not very much different.

The author is highly thankful to Prof. R. P. Rastogi and Dr Kehar Singh of the University of Gorakhpur for their valuable suggestions and encouragement.

References

1. VETO, F., *Acta biochem. biophys. Acad. Hung.*, **1** (1966), 203; **2** (1967), 95.
2. VETO, F., *Acta biochem.*, **2** (1960), 441.
3. ALAXANDER, K. P. & WIRTZ, K., *Z. phys. Chem.*, **195** (1950), 165.
4. HAASE, R. & STEINERT, C., *Z. phys. Chem.*, **21** (1959), 270.
5. RASTOGI, R. P. & BLOKHRA, R. L., *Trans. Faraday Soc.*, **60** (1964), 1386.
6. RASTOGI, R. P. & SINGH, K., *Trans. Faraday Soc.*, **62** (1966), 1754.
7. KEDEM, O. & DARLEL, M. S., *J. phys. Chem.*, **79** (1975), 336.
8. RASTOGI, R. P., SINGH, K. & SHUKLA, P. C., *Indian J. Chem.*, **9** (1971), 1372.
9. RASTOGI, R. P., SHUKLA, P. C. & YADAV, B., *Biochim. biophys. Acta*, **249** (1971), 454.
10. CARR, C. W. & SOLLNER, K., *J. electrochem. Soc.*, **109** (1962), 616.
11. KATCHALSKY, A. & CURRAN, P. F., *Non-equilibrium thermodynamics in biophysics* (Harvard University Press, Cambridge, USA), 1967.
12. RASTOGI, R. P. & SINGH, K., *Trans. Faraday Soc.*, **63** (1967), 2917.

Enhancement of the Power Output of Photogalvanic Cells

P. V. KAMAT, M. D. KARKHANAVALA & P. N. MOORTHY
Chemistry Division, Bhabha Atomic Research Centre
Bombay 400085

Received 6 July 1976; accepted 21 October 1976

It is shown that the power output of photogalvanic cells is limited by their high internal resistance which cannot be reduced by reducing the ohmic resistance alone, e.g. by addition of inert electrolytes. To overcome this difficulty heterogeneous cells have been employed wherein an internal bias potential is provided by an appropriate redox couple in the dark compartment. The net power output obtainable in such cells is at least a factor of ten higher as compared with that obtainable in homogeneous cells hitherto employed. A few other advantages of the heterogeneous cell over the homogeneous one are also indicated.

INVESTIGATIONS of photoelectric chemical phenomenon have, in recent years, assumed great practical importance in view of their possible application to the direct conversion of solar energy into electricity. After the pioneering work of

Becquerrel¹ a big breakthrough was achieved when Rabinowitch² discovered that the photochemical reduction of dyes of the thiazine class such as thionine was, under certain conditions, fully reversible and was accompanied by appreciable (up to 0.3 V) changes in the potential of an inert platinum electrode immersed in the solution. More recently Gomer³ has considered in detail the theoretical aspects of these photogalvanic phenomena, while Potter and Thaler⁴ have evaluated experimentally the power efficiencies of ferrous-thionine photogalvanic cells of the type (A).

In such homogeneous cells they have found the power efficiency to be of the order of $3 \times 10^{-4} \%$ under the most optimum conditions. The usable power output of such photogalvanic cells is limited by their high internal resistance (R_i). Potter and Thaler⁴ have suggested that R_i can be considered to be the sum of the ohmic resistance (R_0) and a contribution (R_p) due to polarization at the photoelectrode. The latter arises as a result of the slowness of discharge of the reduced dye species at the photoelectrode as compared to the homogeneous reaction leading to its destruction.

We have undertaken the investigation of photogalvanic phenomena in various dye redox systems with the objective of improving their power outputs. The important findings are briefly reported here; full details will be published elsewhere.

In homogeneous cells of type-A, R_i (as evaluated by the procedure described by Hann *et al.*⁵ has been found to be ~ 9 kohms, whereas the ohmic resistance of the cell in darkness (as measured by an a.c. conductivity bridge) was 1 kohm. It has been observed that reduction of the latter alone by addition of inert electrolytes such as KNO_3 , Na_2SO_4 or KCl did not improve the power output (Table 1), since although R_0 decreased in the presence of the inert electrolytes as expected, R_i and R_p showed an opposite trend, and hence a reduced power output.

Pt/Fe ²⁺ , Fe ³⁺ , dye, H ⁺ (dark)		H ⁺ , dye ⁻ , dye, Fe ²⁺ , Fe ³⁺ /Pt (illuminated)
(A)		
Pt/Fe ²⁺ , Fe ³⁺ , H ⁺ (dark)		Agar KCl bridge H ⁺ , Fe ²⁺ , Fe ³⁺ , Dye ⁻ /Pt (illuminated)
(B)		

An attempt was, therefore, made to overcome the above problem by providing an internal bias potential (dark potential). The contribution from this bias potential to the power output of the cell was negligible. These experiments were carried out in heterogeneous cells of the type (B). The optimum composition in the illuminated compartment was determined by separate experiment using the homogeneous cell (A) and was found to be: $[\text{Thionine}] = 5 \times 10^{-5}M$, $[\text{Fe}^{2+}] = 5 \times 10^{-3}M$, $[\text{Fe}^{3+}] = 1.5 \times 10^{-4}M$ and $pH = 2$ (H_2SO_4). The composition of the dark compartment was varied as shown in Table 2.

With this arrangement R_p and hence also R_i were found to decrease considerably, resulting in an increased power output. The enhancement in the power output was found to be dependent on the internal bias potential, which in turn was governed by the difference in the $[\text{Fe}^{3+}]/[\text{Fe}^{2+}]$ ratio in the two compartments. In the above series of experiments, where the $[\text{Fe}^{3+}]/[\text{Fe}^{2+}]$ ratio was maintained constant at ~ 0.04 in the illuminated compartment and increased in the dark compartment, the maximum power output derivable was found to attain a limiting value of $\sim 10 \mu\text{W}$ at high $[\text{Fe}^{3+}]/[\text{Fe}^{2+}]$ ratio. This limiting value was about *ten times* higher than the power output obtainable in the homogeneous cell under otherwise similar experimental conditions.

It thus appears that the heterogeneous cell affords significantly higher power outputs; by suitable choice of the photoactive agent, the redox electrolyte

TABLE 1 — CHARACTERISTICS OF HOMOGENEOUS FERROUS-THIONINE PHOTOGALVANIC CELLS

[Incident light intensity (total above 400 nm) = 130 mW/cm²; electrodes: bright Pt foil (each 4 cm²); cell composition: $[\text{Thionine}] = 5 \times 10^{-5}M$, $[\text{Fe}^{2+}] = 5 \times 10^{-3}M$, $[\text{Fe}^{3+}] = 10^{-4}M$, $pH = 2$ (H_2SO_4) (oxygen-free solution); open circuit cell voltage (V_0) in the dark ~ 2 mV]

Inert electrolyte and concn	V_0 on illumination (mV)	Max. power μW	R_i	R_0 (kohm)	R_p
Nil	170	1.0	8.7	0.8	7.9
0.25M KNO_3	150	0.54	11.2	0.2	11.0
0.5M Na_2SO_4	160	0.42	13.1	0.1	13.0
0.5M KCl	85	0.12	15.3	0.08	15.2

TABLE 2 — CHARACTERISTICS OF HETEROGENEOUS FERROUS-THIONINE PHOTOGALVANIC CELLS

[Incident light intensity (total above 400 nm) = 130 mW/cm²; electrodes: bright Pt foil (each 4 cm²); composition of illuminated compartment: $[\text{Thionine}] = 5 \times 10^{-5}M$, $[\text{Fe}^{2+}] = 5 \times 10^{-3}M$, $[\text{Fe}^{3+}] = 10^{-4}M$, $pH = 2$ (H_2SO_4) (oxygen-free solution)]

Dark compt composition ($pH 2$; H_2SO_4)		V_0 dark (mV)	V_0 on illumination (mV)	ΔV (mV)	*Max. power μW	R_i	R_0 (kohm)	R_p
$[\text{Fe}^{2+}]$ ($10^{-4}M$)	$[\text{Fe}^{3+}]$ ($10^{-4}M$)							
50	1	5	180	175	1.3	6.1	1.1	5.0
50	10	66	242	176	5.1	3.0	1.0	2.0
50	250	108	286	178	6.7	2.6	0.7	1.9
50	1000	132	306	174	8.8	2.5	0.7	1.8
100	1000	112	290	178	7.6	2.6	0.5	2.1
20	1000	150	318	168	9.4	2.7	0.7	2.0
5	1000	182	342	160	9.5	2.7	0.7	2.0
1	1000	208	370	162	10.9	3.0	0.7	2.3

*Corrected for contribution from dark potential.

and the bridge separating the two compartments further improvements should be possible. The other advantages of the heterogeneous cells are: (i) the dark compartment need only be formally dark; it need not be protected from light since there is no photoactive material therein; (ii) whereas the homogeneous cell does not permit use of higher $[\text{Fe}^{3+}]/[\text{Fe}^{2+}]$ ratios than the one chosen in the above experiments (Table 1), as at higher Fe^{2+} concentration the open circuit cell voltage itself decreases², there is no limitation on the composition of the dark compartment; and (iii) with the heterogeneous cell it should also be possible to store the light energy in the form of chemical free energy and then release it by discharging through an external load.

We are grateful to Dr K. N. Rao of this Division for helpful discussion and comments.

References

1. BECQUEREL, E., *C.r. heb'd. Acad. Sci. Paris*, **9** (1839), 561.
2. RABINOWITCH, E., *J. chem. Phys.*, **8** (1940), 551, 560.
3. GOMER, R., *Electrochim. Acta*, **20** (1975), 13.
4. POTTER, A. E. & THALER, L. H., *Solar Energy*, **3** (1957), 1.
5. HANN, R. A., READ, C., ROSSEINSKY, D. R. & WASSEL, P., *Nature Lond.*, **244** (1973), 126.

Effect of Temperature & Concentration on Dissolution Potentials of Sodium Chloride, Bromide & Iodide

H. L. GIRDHAR & R. P. MATTA

Department of Chemistry, Kashmir University, Srinagar 6

Received 17 April 1976; accepted 3 December 1976

Dissolution potential and diffusion potential of NaCl, NaBr and NaI have been measured at different temperatures and at different concentrations at 25°. True dissolution potential decreases and diffusion potential increases linearly with increasing temperature. The concentration dependence of diffusion potential has been discussed on the basis of Planck equation and an empirical relation for the variation of true dissolution potential with concentration is given.

DESPITE a good amount of experimental data on the dissolution potential of electrolytes¹⁻⁴, there is still no generalized mechanism for the

origin of such an effect because of the complexity of the phenomenon. Recently^{2,5,6} the sign and magnitude of dissolution potential have been explained on the basis of the formation of electrical double layer at the solid/liquid interface. The dissolution potential has also been found^{3,7} to be influenced by the temperature of solvent and the concentration of the dissolved electrolyte. The purpose of the present study is to explain quantitatively the temperature and concentration dependence of true dissolution potential and diffusion potential of sodium halides.

Analytical reagent grade chemicals were used. All the measurements were made in deionized water prepared by using Elgastat B105 deionizer. As reported earlier⁸, the main contributions towards the observed dissolution potential are (i) true dissolution potential and (ii) diffusion potential that develops due to the formation of concentration gradient when electrode loaded with wet crystals is dipped into the cell. In order to find out the contribution of the diffusion potential to the overall observed dissolution potential it was also measured separately. The details of the experimental technique for measuring the observed dissolution potential and the diffusion potential have already been described⁸. The potentials were measured within an accuracy of ± 2 mV with respect to the clean platinum electrode dipping in the cell. The desired temperature was controlled with an accuracy of $\pm 0.1^\circ$. The concentration dependence was studied at $25^\circ \pm 0.1^\circ$ by measuring the potential in electrolytic solutions of different concentrations.

The potentials measured at different concentrations are given in Table 1 and their variation with temperature is shown in Figs. 1 and 2.

For the same electrolyte solutions at two different concentrations (C_1 and C_2) the diffusion potential is given by Planck equation⁹.

$$\text{Diff. pot.} = \frac{RT}{F} \left(\frac{u_+ - u_-}{u_+ + u_-} \right) \ln \frac{C_1}{C_2} \quad \dots(1)$$

where u_+ and u_- are the ionic mobilities. At a particular temperature, the concentration C_1 of the saturated diffusing solution is constant which is the condition of our experimental measurement of diffusion potential, Eq. (1) reduces to

$$\text{Diff. pot.} = A - B \ln C_2 \quad \dots(2)$$

TABLE 1 — EFFECT OF CONCENTRATION ON DISSOLUTION POTENTIAL AT 25°C

Concentration (g eq/lit)	Sodium chloride			Sodium bromide			Sodium iodide		
	Obs. dissoln pot. (mV)	Diff. pot. (mV)	True dissoln pot. (mV)	Obs. dissoln pot. (mV)	Diff. pot. (mV)	True dissoln pot. (mV)	Obs. dissoln pot. (mV)	Diff. pot. (mV)	True dissoln pot. (mV)
0.0000	-120	-40	-80	-238	-70	-168	-380	-112	-268
0.0001	-110	-38	-72	-230	-68	-162	-268	-100	-168
0.001	-92	-36	-56	-214	-66	-148	-250	-90	-160
0.005	-82	-34	-48	-202	-64	-138	-236	-86	-150
0.01	-74	-30	-44	-194	-60	-134	-232	-72	-160
0.05	-64	-22	-42	-192	-52	-140	-226	-60	-166
0.1	-60	-20	-40	-180	-40	-140	-220	-54	-166
0.2	-50	-14	-36	-170	-36	-134	-210	-44	-166